



Journal of Applied Sciences

ISSN 1812-5654

science
alert

ANSI*net*
an open access publisher
<http://ansinet.com>

The Importance of Corona Effect in Lightning Surge Propagation Studies

M.Z.A. Ab Kadir, W.F. Wan Ahmad, J. Jasni and H. Hizam
Department of Electrical and Electronics Engineering, Universiti Putra Malaysia,
43400 UPM Serdang, Selangor, Malaysia

Abstract: This research focuses on the simulation of the effect of corona model on different conductors used in transmission line design when subjected to the lightning surge. The paper details the procedures used in modelling the corona, as well as the implementation in the PSCAD/EMTDC software for surge propagation studies. There are many models available range from a simple and fixed capacitance to the more complex voltage-dependent capacitance. The corona used for this study is modelled based on the approached relationships and the analyses were done by comparing the results with other models for different types of conductors. The travelling voltage is then measured at different point-of-interest (POI) and compared in terms of the steepness and magnitude for different conductors.

Key words: Corona model, PSCAD/EMTDC, lightning, travelling waves

INTRODUCTION

Corona effect plays an important role in determining the distortion and attenuation of the surges travelling along overhead transmission lines. The corona effect begins when the voltage on the conductor exceeds the corona inception voltage and gives rise to an electric field, which results in increasing the line capacitance as the effective conductor radius grows. IEEE assumes that the effect of corona occurs for the entire voltage waveshape while the CIGRE method totally neglects all effects of corona. Previous results by other workers (de Jesus and de Barros, 1994; Carneiro and Marti, 1991; Nucci *et al.*, 2000; Gallagher and Dudurych, 2004; Podporkin and Sivaev, 1997) have shown that corona effect only occurs when the voltage is increasing and not on the wavetail. This process is shown in Fig. 1.

A sensitivity analysis by Hileman (1999) on a 230 kV double circuit line showed that the backflashover rate (BFR) is higher for a 70 m tower with corona compared to the same tower height without a corona. Therefore, he concluded that conservative values are obtained when neglecting corona and for high towers, the corona effect should be included in the calculations or analyses. He also stated that IEEE over estimates the effect of corona and in contrast, CIGRE should include the effect of corona in the analysis.

Therefore, the objective of the study is to model a corona based on the relationships given by Gary *et al.* (1990) and thus analyse the effect of corona on the

travelling waves. This will be done by stressing the different types of conductors, which is used by the utilities, with the lightning surge and measuring the travelling voltage at point-of-interest (POI). The analysis is particularly important in assessing the steepness and magnitude of the travelling waves as it enters the substation.

OVERVIEW OF PREVIOUS CORONA MODELS

As mentioned earlier, the charge-voltage diagram or q-v curve can be used to characterize the corona phenomenon. Nucci *et al.* (2000) stated that the corona is taken into account by means of dynamic capacitance describing a charge-voltage (q-v) diagram.

Much research have been carried out in evaluating corona models in EMTP. These models range from basic circuit models with diodes, resistors and capacitors to mathematical descriptions of the q-v characteristics. A comparative study has been performed by Carneiro (1988) on some corona models and their implementation in the EMTP. However, a major difficulty encountered using EMTP is assessing the performance of the various approaches against experimental test results.

Although the results derived from experimental studies are available in the literature, a consistent set of measurements, containing all the information needed to validate corona models propagation studies, is not yet available. To approximate the distributed nature of corona, the corona model is connected at the junctions of short

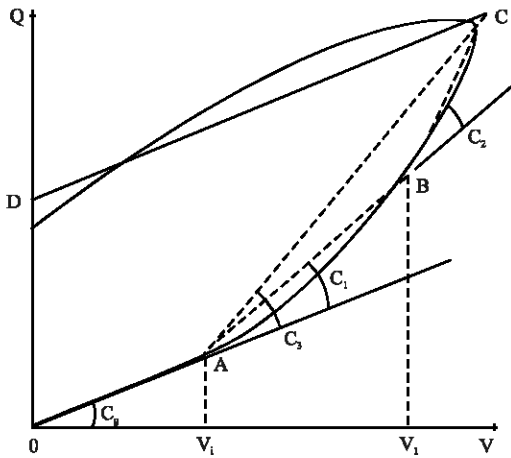


Fig. 1: Typical q-v characteristics and example of linear approximations. C_g = geometric capacitance of the conductor; V_i = corona inception voltage; V_1 = increment voltage at point B as the capacitance increases; $C_1 = C_2 = C_3$ = incremental capacitances (Carneiro and Marti, 1991)

line segments. Wagner and Lloyd (1955) and Kudyan and Shih (1981) have represented the line using very short lumped-parameter π sections, typically 3 to 8 m for lightning surges, but the preferred approach has use of distributed parameter sections, which are much longer length, of the order of 50 to 100 m for lightning surges.

Wagner and Lloyd (1955) and Kudyan and Shih (1981) have proposed lumped equivalent models, as shown in Fig. 2 and 3 respectively, for the analysis. The case was tested using a positive surge that was applied from line to ground. The line was represented by a number of distributed parameter sections and the corona branches, connected to each node, using a standard diode, resistor, capacitor and DC source available in the ATP.

The resistor and capacitor represent the corona energy loss process and change in capacitance of line. Whilst the DC source in these circuits represents the corona inception voltage. Below the corona inception voltage level, C_c is prevented from charging by the diode, maintaining the total line/natural capacitance, C_g (Chowdhuri, 1996). Carneiro and Marti (1991) concluded that the shunt resistor did not affect the response of the model. From their experiments on the use of different values of resistors, the results were identical for all cases. Therefore, they removed the resistor from the corona network.

Carneiro and Marti (1991) state that the corona segment length should be 100 to 50 m. From their experiment, substantial differences are apparent for the

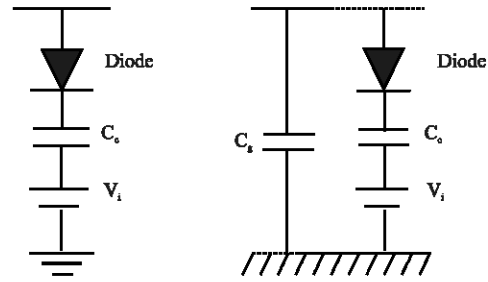


Fig. 2: Corona equivalent circuits proposed by Wagner and Lloyd (1955)

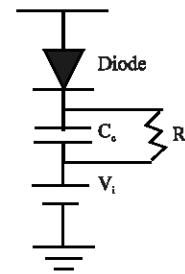


Fig. 3: Corona equivalent circuit proposed by Kudyan and Shih (1981)

lengths between 200 to 100 m, but the differences are small from 100 to 50 m. The transmission line must therefore be divided into a large number of sections. This is important in order to get the accurate results. For example, for a study of lightning surge propagation on a 3 km transmission line, 60 sections of 50 m should be used instead of three sections of 1 km.

They also concluded that the dynamic Suliciu model gives better accuracy than the piecewise linear model. This model was proposed by Suliciu and Suliciu (1981) based on the observation that Q-V curve is significantly affected by the rate of rise of the applied voltage. In Suliciu's model, the corona current is given by:

$$i_c = \frac{dq_c}{dt} = \begin{cases} 0 & \text{if } g_2 \leq 0 \\ g_2 & \text{if } g_1 \leq 0 \\ g_1 + g_2 & \text{if } 0 < g_1 \end{cases} \quad (1)$$

where, $g_j = k [(C_j - C_0)(v(t) - v_1) - q_c]$, $j = 1, 2$ and $C_2 > C_1 > C_0$; $v_1 \geq v_2$; $k_1, k_2 > 0$

In the expression above, C_0 is the geometric capacitance of the line and the remaining parameters are identified by fitting a set of measured Q-V curves (Suliciu and Suliciu, 1981).

MODELLING PROCEDURES

Corona inception voltage (V_i): The corona inception voltage for a single conductor can be estimated from the equation:

$$V_i = \frac{Z_0 E_c}{60} \text{ kV} \tag{2}$$

where, $Z_0 = 60 \ln 2h/r$, is the natural or non corona surge impedance (Hileman, 1999), r is the conductor radius in cm and E_c is the critical gradient usually in kV cm^{-1} .

From the equation above, it is shown that a smaller radius r will lower the inception voltage V_i . There are several empirical formulae in determining the critical gradient, E_c . Below are three well-known formulae proposed by CIGRE, Skilling-Dykes and Peek for calculation of this parameter.

$$E_c = 23 \left(1 + \frac{1.22}{d^{0.37}} \right) \text{ kV cm}^{-1} \text{ CIGRE (1991)} \tag{3}$$

$$E_c = 23 \delta^{0.67} \left(1 + \frac{0.3}{\sqrt{r}} \right) \text{ kV cm}^{-1} \text{ Skilling and Dykes (1954)} \tag{4}$$

$$E_c = 30 m \delta^{0.67} \left(1 + \frac{0.3}{\sqrt{\delta r}} \right) \text{ kV cm}^{-1} \text{ Peek (2007)} \tag{5}$$

where, δ is the relative air density (and usually set to 1 for air) and m is the surface roughness constant with a value of 0.82 (Podporkin and Sivaev, 1997). δ , the relative air density, is important as it determines the inception voltage. When δ is high, the inception voltage is also high and vice versa. The value of δ is determined by the pressure, P and temperature, T . As the temperature and/or pressure changes, the value of δ also changes.

For bundle conductors, Skilling and Dykes (1954) have provided an equation for the equivalent radius r_{eq} , which should be substituted into (4) for the conductor radius, where

$$r_{eq} = \frac{\pi r}{1 + 2(n-1) \sin \frac{\pi r}{nA}} \tag{6}$$

$$\approx \frac{\pi r}{1 + 2(n-1) \frac{\pi r}{nA}} \approx nr$$

where, A is the subconductor spacing in cm and n is the number of subconductors. Approximately, the equivalent radius is equal to n times the conductor radius.

Geometric or natural capacitance, C_g: From the Q-V curve in Fig. 1, as the voltage on the line conductor is increased from zero, the charge on the conductor initially increases linearly, signifying that the capacitance is the constant slope of the Q-V curve (Chowdhuri, 1996). This capacitance, C_g is called the natural (Wagner and Lloyd, 1955) or the geometric capacitance (Gary *et al.*, 1990) for single conductor of the line, which is given by:

$$C_g = \frac{10^{-9}}{18 \ln \frac{2h}{r}} \text{ F m}^{-1} \text{ (Hileman, 1999)} \tag{7}$$

where, h is the height of the conductor above ground.

Dynamic capacitance, C_d: The slope of the Q-V curve results from the dynamic capacitance of the line, C_d which is a variable capacitance and is a function of the applied voltage above the corona inception level (Chowdhuri, 1996). Based on a parabolic relationship as proposed by Gary *et al.* (1990), the slope of the Q-V curve, the dynamic capacitance, can be obtained from the equation:

$$C_d = V_i C_g \left(\frac{V}{V_i} \right)^{B-1} \tag{8}$$

where, B is the empirical parameter given in Table 1.

Empirical equation for charge, q: Gary *et al.* (1990) and Podporkin and Sivaev (1997) have developed empirical equations for the overhead line charge. These equations are useful to plot the Q-V curve that can be used to characterize the corona phenomenon, but not useful in simulations directly.

$$q = q_i V^{(1.17 + V_i^{-0.87})} \text{ Podporkin and Sivaev (1997)} \tag{9}$$

$$q = V_i C_g \left(\frac{V}{V_i} \right)^B \text{ Gary et al. (1990)} \tag{10}$$

Where:

- $V^* = V/V_i$
- $a = 0.08$ (positive impulse)
- $= 0.036$ (negative impulse)
- $q_i = C_g V_i$ Podporkin and Sivaev (1997)

CASE STUDY

Figure 4 is used in this section to model and analyse the effect of corona on the transmission line. The relationship originally proposed by Gary *et al.* (1990) and later adopted by Naredo *et al.* (1995), is used to model a corona in PSCAD/EMTDC.

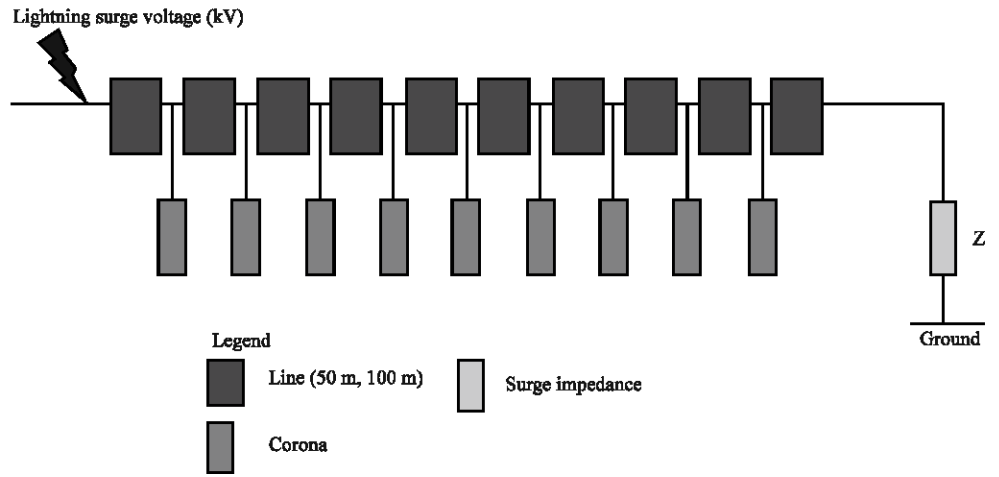


Fig. 4: System modelled to study the effect of the corona on transmission line

Table 1: Value for empirical parameter, B with r, the conductor radius in cm and n, the number of subconductors

Conductor type	B	
	Positive polarity	Negative polarity
Single	0.22r+1.12	0.07r+1.12
Bundle	1.52-0.15 ln (n)	1.28-0.08 ln (n)

$$C_d = \begin{cases} C_g & V \leq V_i, \partial V / \partial t > 0 \\ C_g B \left(\frac{V}{V_i} \right)^{B-1} & V_i \leq V, \partial V / \partial t > 0 \\ C_g & \partial V / \partial t < 0 \end{cases} \quad (11)$$

The relationship shows that all the capacitances below the inception voltage are considered as a geometric capacitance, C_g . Whilst for the voltage above the inception voltage V_i , the capacitance can be determined as above. As shown in Fig. 1 of q-v curve, CD is a discharging process after corona effect on transmission line and is only caused by the geometric capacitance. According to Podporkin and Sivaev (1997), this line is just parallel with OA, showing that there is no more voltage increasing with respect to time where the capacitance is equal to C_g . Therefore, the third condition in equation will not be fulfilled in the corona model.

RESULTS AND DISCUSSION

Figure 5 shows two curves obtained from two different formulae, namely Gary *et al.* (1990) and Podporkin and Sivaev (1997). Line OA initially shows the geometric capacitance, C_g and after the voltage exceeds the corona inception voltage at point A, the gradient increases due to the effect of corona capacitance, C_c . Line BD and CE are parallel with OA and show that the capacitance is equal to C_g when the applied voltage starts reducing.

Table 2: Geometric capacitance for different conductors (assuming a line height of 8.5 m)

Name	Radius (cm)	V_i (kV)	C_g (pF m ⁻¹)
Ferret	0.45	132	6.74
Rabbit	0.50	142	6.84
Horse	0.70	183	7.13
Lynx (275 kV)	0.98	234	7.45
Panther	1.05	247	7.52
Zebra (400 kV)	1.43	312	7.85

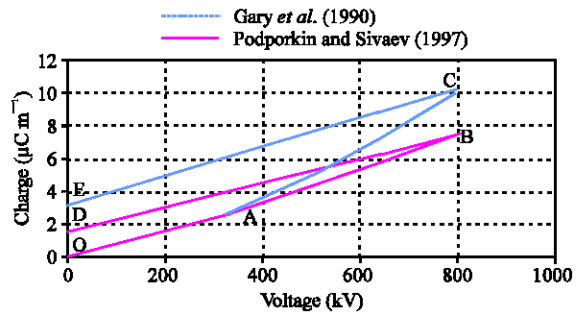


Fig. 5: Typical q-v curve obtained from 400 kV conductor (ZEBRA) at conductor height above ground, h = 8.5 m and peak voltage, $V_p = 800$ kV

For the corona inception voltage calculations, the overall radius of the conductor has been used without accounting for stranding, which has been neglected. The results above would be lower if the stranding of the conductor is considered, due to the ‘sharper edges’ of the strands. In other words, the conductors with the strands give higher electric fields in comparison with the solid conductor (without strands) and therefore the inception voltage is reduced. Table 2 shows some calculations of the inception voltage and geometry capacitance for different type of conductors. It is clearly shown that for the larger conductor radius, a smaller inception voltage and geometric capacitance can be obtained.

Table 3: Comparison of the corona inception voltage (V_i)

Conductor	Radius (cm)	E_c (kV cm ⁻¹)			V_i (kV)		
		Skillings-Dykes	CIGRE	Peek	Skillings-Dykes		
					Dykes	CIGRE	Peek
Ferret	0.45	33.29	52.18	35.60	123	193	132
Rabbit	0.50	32.76	51.06	35.04	133	208	142
Horse	0.70	31.25	47.78	33.42	171	260	183
Lynx	0.98	29.97	44.88	32.42	219	328	234
Panther	1.05	29.73	44.32	31.82	231	344	247
Zebra	1.43	28.80	42.02	30.77	292	425	312

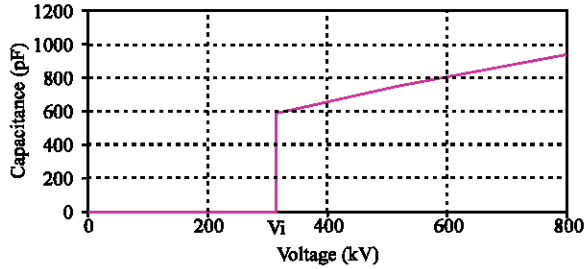


Fig. 6: Corona capacitance versus voltage amplitude for ZEBRA conductor with a radius of 1.43 cm for 50 m segment. System modelled based on Fig. 4

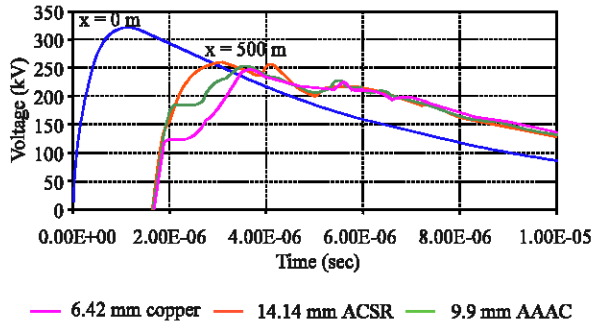


Fig. 7: Effect of conductor radius on surge propagation along transmission lines with $L = 50$ m. System modelled based on Fig. 4

The results in Table 3 show that the values calculated using the CIGRE equation are significantly different compared to both Skillings-Dykes and Peek. The difference between the variable capacitance (non-linear) and fixed capacitance (linear) is the corona capacitance. The corona capacitance increases with instantaneous applied voltage after it exceeds the corona inception voltage, which is 312 kV. The line segment is 50 m (Fig. 6).

Figure 7 shows the effect of conductor types and radius on surge propagation. After 500 m, the result shows that the effect of corona on the rise time for copper is greater compared to the ACSR and AAAC. The main reason is the size of conductor used in copper is smaller than ACSR and AAAC.

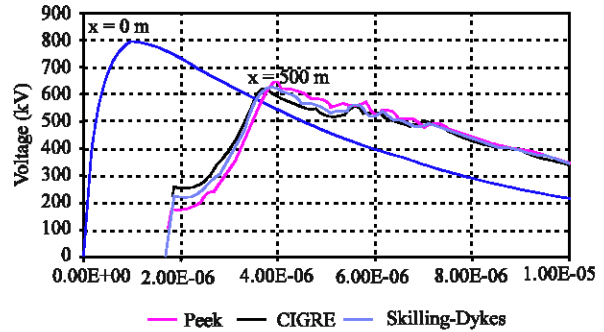


Fig. 8: Effect of inception voltage, V_i obtained from different formulae with $h = 19.43$ m, $r = 0.98$ cm and $V_p = 800$ kV

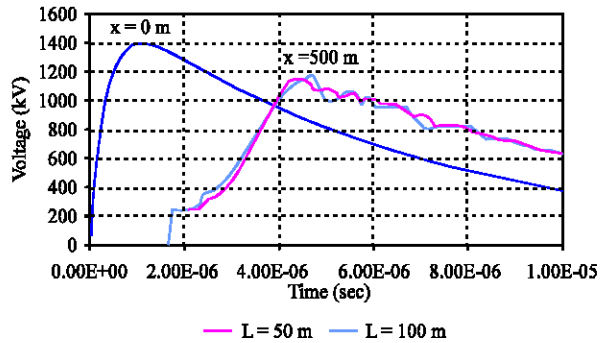


Fig. 9: Surge propagation on 275 kV line. Influence of section length

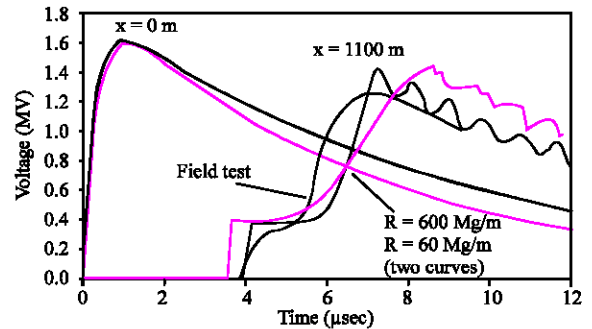


Fig. 10: Comparison between the implemented model and Carneiro and Marti model

As shown in Table 2, the use of different formulae to obtain the corona inception voltage tends to give different results when different corona models are included on the line. Figure 8 shows three different curves: pink for Peek, black for CIGRE and blue for Skillings-Dykes. A low critical gradient E_c results in a lower inception voltage. As a result, the formula proposed by Peek gives greater reduction in the steepness of the waveform compared with the CIGRE and Skillings-Dykes formulae.

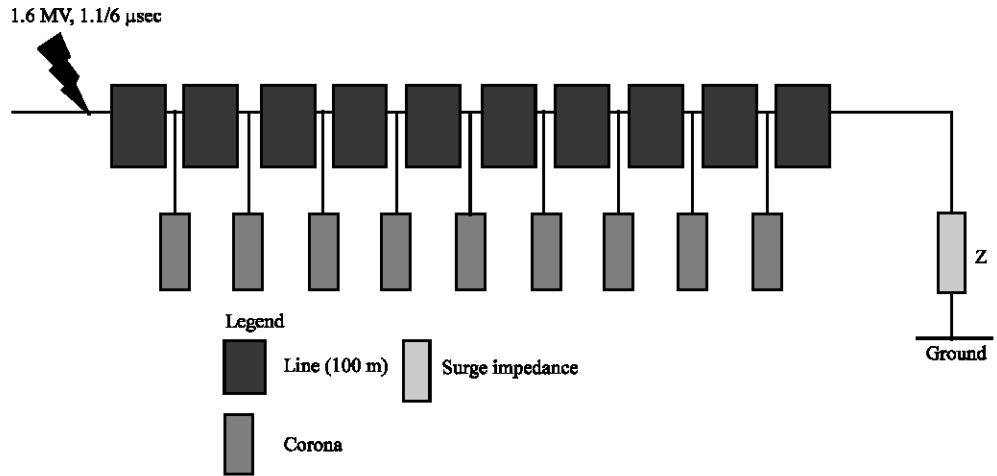


Fig. 11: System modelled for Tidd line comparison

The effect on rise time for instance is important when considering the coordination gap (CG) that are used to protect the transformer. By having a steep fronted waveform, a CG will not have enough time to react and hence can damage the transformer. Therefore, this steepness reduction will provide some time for a CG to react properly.

As mentioned by Carneiro and Marti (1991), the use of a short section length, normally 50 to 100 m is important in corona investigation. As shown in Fig. 9, after 500 m of surge propagation, the use of a 50 m section length provides a smooth waveform compared to the results from the use of a 100 m length. The result also shows that there is a small reduction in magnitude of the peak voltage and steepness of wave front when a 50 m section length was used.

Figure 10 shows a comparison made between the present model (non-linear) and the Carneiro and Marti (1991) model on a 345 kV Tidd line, which is connected to Canton Central in Ohio, USA. The purpose is to compare with the results obtained by Wagner and Lloyd (1955). Investigations on this Tidd power line have been carried out by many researchers (Kudyan and Shih, 1981; Xiao-rong *et al.*, 1989; Carneiro *et al.*, 1994) over a long period of time. All the parameter values used for this simulation were obtained from their respective publications. The values used were 1.16 cm for the conductor radius, 6.73 pF m^{-1} for the geometry capacitance, 22.6 m for line height and 1100 m for the line length. Based on these parameters, the corona inception voltage is calculated to be approximately 386 kV. Figure 11 shows the system modelled for this comparison.

Figure 10 shows six curves: the black curves are Carneiro and Marti's curves (input surge, field test result and two curves of the model with the resistor). The pink

curves are the estimated input and the output for the implemented corona model 1100 m down the line respectively. Although the magnitude of the peak voltage is not significantly different, it has reduced the steepness and changed the waveform. This result shows that the present model gives a good solution for modelling the corona effect on the transmission line.

CONCLUSION

This research has presented in details related to the modelling procedures and effect of corona model on different types of conductors, which are different in conductor radius and inception voltage. The results obtained from the simulations showed that the effect of corona model on the transmission line, particularly during the lightning, should be considered as it will reduce the magnitude and steepness of the surge overvoltage. As far as the insulation coordination studies are concerned, the presence of corona model in the studies could influence the results obtained and therefore, it is suggested that the corona model should be included in the analysis. The analyses have demonstrated that the different conductor sizes and types will give variations in results and this is particularly true considering the different types of conductors used by the utilities for their transmission lines. Recent publications by the authors, with the inclusive of corona model in their insulation coordination studies, have given the good results when compared to the published BFR by CIGRE and IEEE (Cotton and Ab Kadir, 2007). Although there is no direct relation between the corona and the BFR, it is believed that the presence of corona model will improve, if not much, the results of the studies. As far as the utility is concerned, these results will also help the designer and protection

engineers to become more aware of the important of including the corona model in their insulation coordination studies.

REFERENCES

- Ab Kadir, M.Z.A. and I. Cotton, 2007. Estimating the probability of transformer damage and backflashover rate using randomised leader progression model. Presented at the World Engineering Congress, August 5-9, Penang, Malaysia, pp: 175-184.
- Carneiro, S., 1988. A comparative study of some corona models and their implementation in the EMTP. CEA Trans. Eng. Oper. Div., 1: 1-26.
- Carneiro, S. and J.R. Marti, 1991. Evaluation of corona and line models in electromagnetic transient simulation. IEEE Trans. Power Delivery, 6: 334-342.
- Carneiro, S., J.R. Marti, H.W. Dommel and H.M. Barros, 1994. An efficient procedure for the implementation of corona models in electromagnetic transients programs. IEEE Trans. Power Delivery, 9: 849-855.
- Chowdhuri, P., 1996. Electromagnetic Transients in Power Systems. 1st Edn. Research Studies Press Ltd., England, ISBN: 0863801803.
- Cotton, I. and M.Z.A. Ab Kadir, 2007. A randomised leader progression model for backflashover studies. Eur. Trans. Elec. Power 10.1002/etep.200.
- CIGRE., 1991. Guide to procedures for estimating the lightning performance of transmission lines. CIGRE Brochure, pp: 63. <http://www.e-cigre.org/Order/select.asp?ID=67>.
- De Jesus, C. and M.T. Correia de Barros, 1994. Modelling of corona dynamics for surge propagation studies. IEEE Trans. Power Delivery, 9: 1564-1569.
- Gallagher, T.J. and I.M. Dudurych, 2004. Model of corona for an EMTP study of surge propagation along HV transmission lines. IEE. Proc. Gener. Transm. Distrib., 151: 61-66.
- Gary, C., G. Dragan and I. Langu, 1990. Impulse corona discharge energy around the conductors. Presented at the Conference Record of the Industry Applications Society Annual Meeting. Oct. 7-12, Seattle, USA., pp: 922-924.
- Hileman, A.R., 1999. Insulation Coordination for Power System. 1st Edn. Marcel Dekker Inc., New York, ISBN: 0824799577 .
- Kudyan, H.M. and C.H. Shih, 1981. A non linear circuit model for transmission lines in corona. IEEE Trans. Power Applied Syst., 100: 1420-1430.
- Naredo, J.L., A.C. Soudack and J.R. Marti, 1995. Simulation of transients on transmission lines with corona via the method of characteristics. IEE Proc. Gener. Transm. Distrib., 142: 81-87.
- Nucci, C.A., S. Guerrieri, Barros and F. Rachidi, 2000. Influence of corona on the voltages induced by nearby lightning on overhead distribution lines. IEEE Trans. Power Delivery, 15: 1265-1273.
- Peek, F.W., 2007. Dielectric Phenomena in High Voltage Engineering. 1st Edn., Gallaher Press, ISBN: 1406783374 .
- Podporkin, G.V. and A.D. Sivaev, 1997. Lightning impulse corona characteristics of conductors and bundles. IEEE Trans. Power Delivery, 12: 1842-1847.
- Skilling, H.H. and P.K. Dykes, 1954. Distortion of travelling waves by corona. AIEE Trans. Power Applied Syst., 73: 196-210.
- Suliciu, M.M. and I. Suliciu, 1981. A rate type constitutive equation for the description of the corona effect. IEEE Trans. Power Applied Syst., 100: 3681-3685.
- Wagner, C.F. and B.L. Lloyd, 1955. Effects of corona on travelling waves. AIEE. Trans. Power Applied Syst., 74: 858-872.
- Xiao-rong, L., O.P. Malik and Z. Zhi-da, 1989. Computation of transmission line transients including corona effects. IEEE Trans. Power Delivery, 4: 1816-1822.